

Towards a Robust Transport Network With Self-adaptive Network Digital Twin

Cláudio Modesto^{a,*}, João Borges^a, Cleverson Nahum^a, Lucas Matni^a, Cristiano Bonato Both^c, Kleber Cardoso^b,
Glaucio Gonçalves^a, Ilan Correa^a, Silvia Lins^d, Andrey Silva^d, Aldebaro Klautau^a

^aLASSE, Federal University of Pará, Belém, 66075-110, Brazil

^bInstitute of Informatics, Federal University of Goiás, Goiânia, 74001-970, Brazil

^cApplied Computing Graduate Program, University of Vale do Rio dos Sinos, São Leopoldo, 93022-750, Brazil

^dEricsson Research, São Paulo, Indaiatuba, 13337-300, Brazil

Abstract

The ability of the network digital twin (NDT) to remain aware of changes in its physical counterpart, known as the physical twin (PTwin), is a fundamental condition to enable timely synchronization, also referred to as *twinning*. In this way, considering a transport network, a key requirement is to handle unexpected traffic variability and dynamically adapt to maintain optimal performance in the associated virtual model, known as the virtual twin (VTwin). In this context, we propose a self-adaptive implementation of a novel NDT architecture designed to provide accurate delay predictions, even under fluctuating traffic conditions. This architecture addresses an essential challenge, underexplored in the literature: improving the resilience of data-driven NDT platforms against traffic variability and improving synchronization between the VTwin and its physical counterpart. Therefore, the contributions of this article rely on NDT lifecycle by focusing on the operational phase, where telemetry modules are used to monitor incoming traffic, and concept drift detection techniques guide retraining decisions aimed at updating and redeploying the VTwin when necessary. We validate our architecture with a network management use case, across various emulated network topologies, and diverse traffic patterns to demonstrate its effectiveness in preserving acceptable performance and predicting quality of service (QoS) metrics under unexpected traffic variation, such as delay and jitter. The results in all tested topologies, using the normalized mean square error as the evaluation metric, demonstrate that our proposed architecture, after a traffic concept drift, achieves a performance improvement in per-flow delay and jitter prediction of at least 64% and 21%, respectively, compared to a configuration without NDT synchronization.

Keywords: Concept drift, graph neural network (GNN), lifecycle management (LCM), twinning.

1. Introduction

Network digital twin (NDT) is a platform designed to aid in the management and automation of physical network communication tasks based on interactions with its virtual counterpart, also called virtual twin (VTwin), at a certain periodicity and fidelity [1, 2]. This relation allows the network operator to emulate different scenarios in network planning to perform a *what-if* analysis [3, 4]. This analysis aims to evaluate the impact of management changes in the network infrastructure when these tests are impossible due to logistical issues or costs that render them unfeasible, such as in production environments [5, 2]. For that reason, this platform is considered an enabling technology to optimize 5th and 6th generation (5G/6G) network communication [2], providing improved solutions to problems such as slicing management [6, 7], routing optimization [8, 9], resource power allocation [3], and admission control [10].

Use of an NDT platform in a production environment can create several challenges, particularly concerning the long-term accuracy of the digital twin (DT). It is essential to account for variability in incoming data, ensuring that the VTwin continually adapts to reflect real-world changes. When we consider a VTwin neural network model to achieve this reliability, such as a graph neural network (GNN) [11], it is fundamental to have a well-defined lifecycle

*Corresponding author.

Email address: cclaudio.barata@itec.ufpa.br (Cláudio Modesto)

management (LCM) that organizes all phases, including the *planning*, *training*, and *operational* aspects of the NDT platform [12, 13, 14]. When a deployed NDT is used during the operational phase, an important research question arises concerning the synchronization between the VTwin and the physical twin (PTwin). Synchronization issues are widely explored in the general context of DTs, considering applications at factory workstations, the industrial Internet of Things, power systems, etc. [15, 16]. However, these questions are rarely explored within the specific context of a transport network NDT based on GNN. Given that the transport network plays a crucial role as the interconnection between the core network and the radio access network (RAN) [7, 17], and the extensive body of literature supporting data-driven approaches using GNN [8] for modeling and representing transport networks, it becomes possible to investigate particular challenges related to twin synchronization, such as the methods used to achieve it and the underlying synchronization patterns [15].

In this sense, we propose an enhanced architecture grounded in the core lifecycle principles of NDT to address these challenges, focusing on maintenance and resilience. The architecture is designed to support a robust platform capable of adapting to traffic variability, also referred to as *covariate drift*, a special case of concept drift [18, 19], which can arise from disruptions such as congestion, unreachable switches, broken links, or shifts in traffic patterns. Our approach emphasizes synchronization between the VTwin and the PTwin aimed to assist data-driven approaches remain up-to-date whenever an input distribution change is detected. We adopted a data-driven synchronization pattern [15] managed through a concept drift detector that monitors network traffic for changes. When significant deviations are detected, a retraining process is triggered to realign the VTwin with the current state of the PTwin. Since our simulations employ a supervised learning setup, where the “ground truth” total delay and jitter are known, we evaluate and validate the generalization performance of the VTwin in the proposed architecture as the PTwin experiences dynamic changes in traffic intensity and patterns. The results of the proposed experiments demonstrate a performance improvement in all tested emulated topologies with different network traffic patterns, using the normalized mean square error (NMSE) as the evaluation metric. This shows that our proposed architecture achieves an improvement in total per-flow delay and jitter prediction of at least 64% and 21%, respectively, after a traffic concept drift. In some other topologies, this improvement is greater than 99% and 98%, respectively. Finally, with these improvements, we propose a final evaluation in a use case application based on service-level agreement (SLA) monitoring to demonstrate the importance of NDT synchronization, considering high-level metrics for network planning, such as the number of SLA violations.

Our main contributions to this article are:

- A novel NDT architecture incorporating LCM principles during the operational phase, such as the re-deployment of an updated VTwin model when necessary. This contribution aimed to assist data-driven approaches (used to predict per-flow delay and jitter) remain up-to-date whenever an input distribution change is detected.
- As part of our architecture, a concept drift detection module is integrated to monitor incoming network traffic features. This NDT module enables the analysis of traffic behavior to make informed decisions about when to update the VTwin model.
- A use case application for network management related to SLA violation prediction compares the performance of the proposed application with and without NDT synchronization.

The remainder of this article is organized as follows: in Section 2 we compare our work with different proposed data-driven NDT in the literature, considering various levels of implementation in the transport network domain and their characteristics related to NDT supported modules, such as the synchronization module. In Section 3, we present the proposed enhanced NDT architecture, taking into account the main functional requirements of NDT, and show the essential building blocks of each, such as the VTwin architecture, the synchronization methods based on concept drift detection techniques, and complementary modules. In Section 4, we detail the experiments conducted to evaluate the proposed methods for twin synchronization and present the key evaluation results across various topologies and traffic patterns, as well as a use case with SLA monitoring. Finally, Section 5 summarizes the main contributions of this work and outlines directions for future research.

2. Related Work

Recent studies point DTs to an important technology for the 5G/6G networks [20, 21, 22, 23, 24]. This aligns with their need to establish reliable environments for developing and testing their critical parts, such as wired environments [10], where DTs can provide excellent support. However, during this wave of adoption, the intersection of DT and networking—still an emerging area of study—led to a diverse range of approaches. Many of these did not align fully with the definitions of an NDT as systematized by standards organizations [25, 26] and industry stakeholders [2, 27]. Consequently, related work found in the literature presents limited analyzes of practical aspects. For example, regarding the system lifecycle or the twinning rates, the latter refers to the rate of synchronization between the PTwin current state and its corresponding representation in the VTwin [28]. More specifically, much of the literature regarding NDTs of the transport domain has focused on using machine learning (ML)/surrogate model-based methods to generate the VTwin. The increase in popularity of this DT approach, which can also be called data-driven [12], can be traced back to the work of Rusek et al. [8], which established the usage of a GNN model called RouteNet for predicting path-level metrics in routing optimization and network upgrade use cases. The usage of this model was further investigated by several works, which were built on the previously established RouteNet [29, 30, 31, 32, 11, 10, 33].

Recently, the work of Ferriol-Galmés et al. [11] utilized a modified version of RouteNet, called RouteNet-Fermi, to model network communication with various topologies, traffic distributions, and queuing configurations, enabling the prediction of packet loss, delay, and jitter. In this work, since all data is provided from a packet-level simulator, there are no two-way interactions between PTwin and VTwin. Therefore, the case presented in the article does not constitute a closed-loop NDT. Moreover, the investigations did not address the possible performance degradation of the VTwin in cases of data and/or concept drifts [34]. In this context, the cases presented in this work and several others built on RouteNet [29, 30, 31, 32, 11] did not address the robustness aspect of an NDT, as they did not explore its lifecycle either.

The exception to this lack of closed-loop implementation in works based on RouteNet is the work of Messaoudi et al. [10], Zalat et al. [35], and Aben-Athar et al. [4], which are, to the best of our knowledge, the first closed-loop environments considering physical layers that interact with an artificial intelligence (AI) model. The works in [10, 4] feed an application module tailored to operate over the physical counterpart defined by virtual switches on Mininet [36]. The work in [35] took the same approach but considered a small-scale physical testbed. However, a noteworthy aspect of this work is that there are elements for twin synchronization that are based on a trigger-based online learning approach. The main difference between this work and our proposed architecture, apart from the use of online learning training, is that the authors specifically focused on exploiting the correlation between the predicted per-flow delay and the ground truth per-flow delay to update the states of the VTwin based on those of the PTwin. This correlation, when applied, can also be considered the simplest form to compare two twin states (outputs) without explicitly using a concept drift detector. However, a key drawback is the requirement for ground-truth labels to start a retraining process. For the other two works, despite closed-loop interactions between the physical and virtual domains, there is no DT lifecycle management controlling the rate at which both parts synchronize and update their respective states, for instance, through a retraining process. In this context, the authors in [10, 4] ran the traffic only once, and after completing it, they performed no further operations to detect whether the VTwin performance would remain acceptable.

In addition to these, other works in the literature either proposed purely GNN-based approaches, such as FlowDT [37] or GNNetSlice [7], or adopted different ML models as their VTwins. For example, Lai et al. [38] adopted a model named eConvLSTM; Shin et al. [39] used GNN along with Long Short-Term Memory (LSTM) and a data extraction approach [40] that uses dynamic graph attention network (DGAT). However, among these other works, only Shin et al. [39] and Yu et al. [40] presented investigations on the NDT LCM, while none presented concept drift implementations.

Finally, in terms of the datasets used in these works, there is a noticeable concentration of studies [6, 30, 7, 39, 31] based on specific datasets derived from the OMNeT++ simulator [41]. This trend presents advantages and limitations. On the one hand, using datasets from a common source provides a stable baseline, enabling fair comparisons across different approaches in terms of generalization performance. On the other hand, relying solely on pre-built datasets limits the exploration of more realistic aspects of NDT, such as the aforementioned closed-loop operations or DT synchronization, as there is no interaction with a real or emulated environment.

Given the current state of the literature on twin synchronization in the transport network domain, Table 1 summa-

rizes the works discussed in this section based on four primary characteristics: (i) closed-loop operation, referring to the interaction between the VTwin and PTwin; (ii) support for concept drift detection to handle traffic variability; (iii) the presence of twin synchronization mechanisms, regardless of whether they explicitly use concept drift detection; and (iv) consideration of NDT LCM elements, such as the planning, training, or operational phases. The comparative analysis in Table 1 emphasizes complementary and essential features of an NDT considered in this work, rather than focusing solely on improving the VTwin model itself, as is common in prior works. In this context, our objective is not to compare different VTwin models but rather to consider a given VTwin model and examine how our proposed architecture aims to preserve its predictive performance through a twin synchronization strategy. Finally, Table 1 considers only studies that explicitly use the term NDT. This decision reflects our intention to maintain terminological consistency. Although other platforms, such as cyber-physical system (CPS) [42, 43], may share certain similarities with NDTs, they often involve broader specifications that extend beyond the scope of NDTs as assumed in our work.

Table 1: Comparison between NDT characteristics of the related works and our proposed architecture with support for concept drift.

Authors	Closed-loop	Concept drift detection support	Twin synchronization	NDT LCM elements
Rusek et al., 2020 [8]	✗	✗	✗	✗
Happ, et al., 2021 [29]	✗	✗	✗	✗
Wang et al., 2022 [6]	✗	✗	✗	✗
Güemes-Palau et al., 2022 [44]	✗	✗	✗	✗
Ferriol-Galmés et al., 2022 [37]	✗	✗	✗	✗
Saravanan et al., 2022 [30]	✗	✗	✗	✗
Lai et al., 2023 [38]	✗	✗	✗	✗
Farreras et al., 2023 [31]	✗	✗	✗	✗
Messaoudi et al., 2023 [10]	✓	✗	✗	✗
Shin et al., 2023 [39]	✗	✗	✗	✓
Yu et al., 2023 [40]	✗	✗	✗	✓
Ferriol-Galmés et al., 2023 [11]	✗	✗	✗	✗
Zalat et al., 2024 [35]	✓	✗	✓	✗
Modesto et al., 2024 [33]	✗	✗	✗	✗
Farreras et al., 2025 [7]	✗	✗	✗	✗
Aben-Athar et al., 2025 [4]	✓	✗	✗	✗
Our work	✓	✓	✓	✓

3. Enhanced Network Digital Twin

The proposed enhanced architecture is divided into the modules illustrated in Figure 1 and shares some inheritance from standardization bodies [25, 26] and industry players [2]. Following a bottom-up description, the first module corresponds to the PTwin defined by the switches in the transport network. Above the PTwin, we have the software-defined networking (SDN) controller and its related interfaces, northbound and southbound. Next to it, we have the VTwin, which in our solution is implemented using a GNN model. It provides a digital representation of the relationship between network traffic and topology links. This model plays a crucial role in estimating the QoS parameters in

the PTwin. Table 2 provides an overview of the terms used to represent both twins. The following module is the data management system, which stores useful features of the traffic database (see Table 3). This module maintains a unified repository of transport network data, which is essential for feeding the VTwin with relevant features in the retraining process. Additionally, this module includes the necessary functions to collect and store traffic data, ensuring seamless integration with the overall system.

Table 2: Description of terms used.

Term	Description
\mathcal{G}	Transport network topology
\mathcal{F}	Set of network flows
\mathcal{V}	Set of nodes
\mathcal{E}	Set of links
O	Source switch
D	Destination switch
e_j	j -th link
f_t	t -th flow
\mathbf{x}_{e_j}	j -th link feature vector
\mathbf{x}_{f_t}	t -th flow feature vector
x	Average traffic rate
T	Total number of flows
J	Total number of links in a path
P_t	Probability distribution at discrete time t
$a(\cdot)$	Attention score
$\psi(\cdot)$	Message function
$\phi(\cdot)$	Update function
θ	Multilayer perceptron (MLP) learnable parameters
\oplus	Aggregation function
O	Readout output
\mathbf{j}	Vector of link indices
\mathbf{i}	Vector of flow indices
K	Number of iteration on message passing
\mathcal{E}'	Path of a specific flow
p_j	j -th link propagation delay
q	Type of QoS metric (delay or jitter)
$y^{(q)}$	per-flow QoS metric
$\hat{y}^{(q)}$	Predicted per-flow QoS metric
m	Flow embedding size
n	Link embedding size
\mathbf{h}	Embedding vector
\mathcal{N}	Neighborhood of a node

Operating in the background to enable communication between these NDT modules, we have the interfaces defined by the SDN controller, which allow for indirect data exchange between the VTwin and the controller. This setup is intended to apply any necessary modifications in the PTwin and facilitate indirect data exchange between the database collector and the PTwin to fulfill this database with updated information from the physical environment. With this closed loop of control and traffic data between both twins, the VTwin predictions can be used in high-level applications, either with the involvement of a network operator, as defined by Aben-Athar et al. [4], or autonomously, without human supervision, as demonstrated by Messaoudi et al. [10]. In this article, we assume an SLA monitoring application. Complementary to this closed loop, the main contribution relies on the modules related to the synchronization of the NDT modules, which are responsible for synchronizing the status of the transport network in both

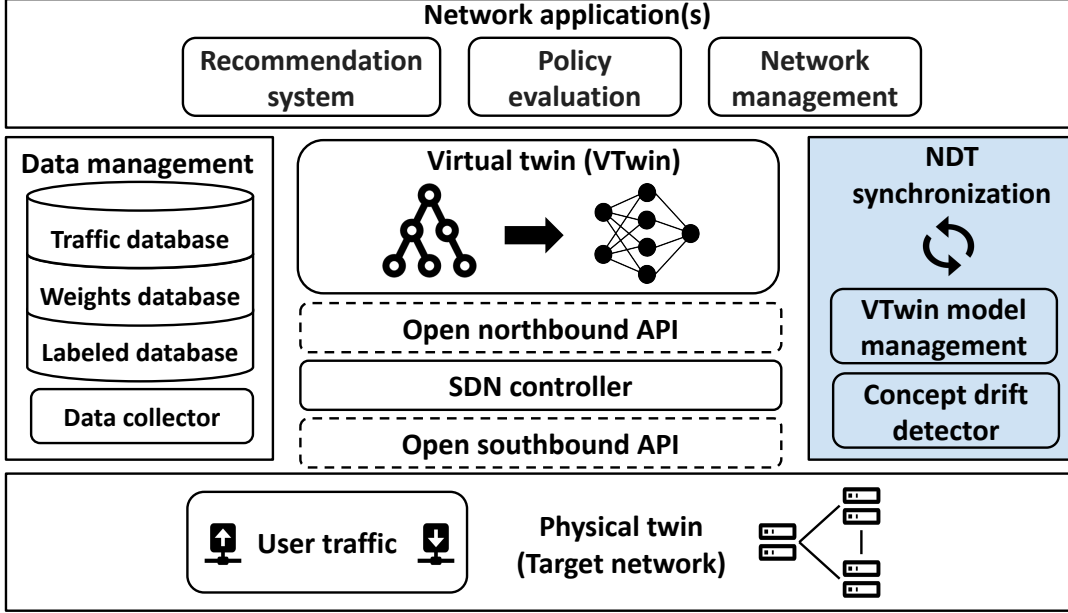


Figure 1: Enhanced NDT architecture to construct a reactive approach against traffic variability. This self-adaptivity is achieved through the proposed implementation of the NDT synchronization functions (in blue), including the concept drift detector and VTwin model management.

domains in a reactive manner. Along with the concept drift detector, this module monitors whether the incoming traffic that reaches the VTwin remains similar. Once changed and detected by the drift detector, this module has the capability to trigger a retraining process, as this change can also mean that the VTwin model is no longer predicting the total per-flow delay or jitter with acceptable error performance. Finally, the source code of the proposed closed-loop architecture, its integration with concept drift techniques, the datasets used, and the evaluation methodology are available in a public GitHub repository.¹

3.1. Physical twin

As the PTwin, we considered a transport network topology modeled as a 2-tuple graph $\mathcal{G} = (\mathcal{V}, \mathcal{E})$. In this graph, \mathcal{V} denotes the set of nodes, each representing a network switch, while $\mathcal{E} \subseteq \mathcal{V} \times \mathcal{V}$ defines the set of edges (i.e., links) that connect pairs of nodes. Within this network, a traffic generator can produce a set of flow traffic instances denoted as $\mathcal{F} = \{f_1, f_2, \dots, f_t, \dots, f_T\}$, with a total of T flows. Each flow instance consumes network resources, such as link bandwidth, by applying variable load intensities along a specific path composed of links $\mathcal{E}' = \{e_1, e_2, \dots, e_j, \dots, e_J\}$, where J denotes the flow length. We also define each flow instance as a tuple $f_t = (\mathbf{x}_{f_t}, O, D, \mathbf{j})$, where $\mathbf{x}_{f_t} \in \mathbb{R}^4$ is a feature vector that characterizes the flow's behavior. In this sense, each feature vector \mathbf{x}_{f_t} is associated with a mapping rule h to a real number defined as the interested QoS metric, such that $h : \mathbf{x}_{f_t} \rightarrow \{y^{(q)}\}$, where $q \in \{\text{delay}, \text{jitter}\}$, and such that y^{delay} and y^{jitter} represent the per-flow delay and jitter, respectively. Furthermore, O and D represent the source and destination switches ($\{O, D\} \in \mathbb{Z}^+$); and \mathbf{j} is a vector of link indices that the t -th flow traverses. Similarly, each link instance is defined as a tuple $e_j = (\mathbf{x}_{e_j}, \mathbf{i})$, where $\mathbf{x}_{e_j} \in \mathbb{R}^2$ is a feature vector describing the link's characteristics, and \mathbf{i} is a vector of flow indices representing the flows traversing that j -th link. The complete list of features for both flow and link instances is provided in Table 3. Among these features, special attention should be given to the propagation delay, which was converted from a link-level feature to a flow-level feature by summing the propagation delays p_j of the j -th links along the path \mathcal{E}' . Furthermore, the average traffic rate $x \in \mathbf{x}_{f_t}$ at time t is modeled as a random variable following a probability distribution P_t , such that $x \sim P_t$.

¹<https://github.com/lasseufpa/robust-ndt>

Table 3: Flow and link features that are extracted to be used as input feature for training and testing the VTwin model.

Feature	Unit	Type
Average traffic rate	bits/s	Flow
Path propagation delay	s	Flow
Flow length	—	Flow
Average packet loss	packets/s	Flow
Capacity	bits/s	Link
Link load	%	Link

3.2. Database management and SDN controller

The database used for the decision-making process is divided into three types of storage. The first one, called the *traffic database*, is related to the data stream that was filtered after the traffic generator created it and will serve as input for the VTwin model to perform the necessary QoS prediction; i.e., the total per-flow delay or jitter labels are unavailable. The second type of database is related to the examples that should be used to retrain our VTwin model, and it is called a *labeled database*, as we manipulated the ground truth delay or jitter to update the VTwin model weights when necessary. The last storage refers to the *weights database*, which is aimed at storing the historical VTwin model weights during the NDT operation. In summary, the primary roles of each database are depicted in Figure 2.

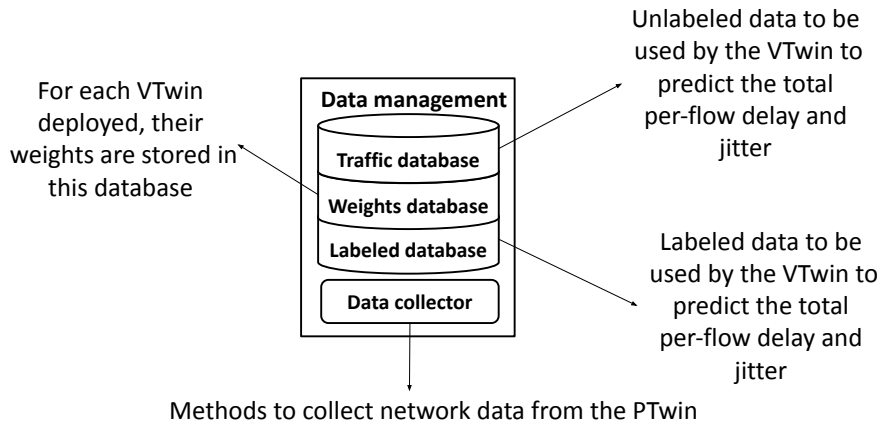


Figure 2: Primary roles of each database in the NDT data management module.

To store this raw data, we are also considering data collection functions to discard unnecessary packet-level traffic data, such as the Internet Protocol (IP) addresses of the server and client and transmission timestamps. Therefore, we aim to store only QoS related features that we can extract from the PTwin environment and that are useful for the VTwin prediction task. It is important to note that we assume the data required for the retraining process has already been collected, labeled, and stored in our database. Furthermore, issues related to synthetic data generation or real-time data collection for retraining are considered outside the scope of this work.

The interfaces employed in the proposed architecture (Figure 1) enable the indirect exchange of control data between both twins, with the SDN controller serving as the network operating system [45]. This type of interaction is similar to that of a controller-based CPS [46, 47, 42], which also leverages SDN controller interfaces to translate high-level network policies into control instructions executed at the physical layer. With this context, we utilize the SDN controller as the central bridging tool, leveraging its available application programming interface (API). Specifically, another feature stored in the traffic and labeled database consists of the vectors \mathbf{i} and \mathbf{j} . Consequently, one of the critical functions of the interface module is to work with the data collection's path collector, which identifies and records the routes taken between each source–destination node pair. The path collector operates based on a specific

node identifier, which is a 16-character hexadecimal string derived from the PTwin. Therefore, given that flow traffic was initialized between two pairs of nodes, it is possible to consult the path of each flow through the controller REpresentational State Transfer (REST) API. In this case, it is assumed that the SDN controller operates in a reactive forwarding manner; that is, it considers forwarding decisions and route establishment on demand, working only when a packet needs to be sent. Proactive forwarding can also be considered in this context by the SDN controller, since this configuration is transparent to VTwin (VTwin only needs to know the path that a given flow traverses). Moreover, for different source destination switch pairs, we assume that the shortest path defines the routing table between them.

3.3. Virtual twin

Considering the adopted NDT architecture, the VTwin assumes a role in mimicking key aspects of its PTwin. In this sense, the VTwin is based on a GNN, a type of deep learning model. Accordingly, the VTwin is responsible for abstracting the most complex organization of the transport network and synthesizing its key aspects to evaluate the interest QoS parameter while maintaining a certain level of fidelity in the physical-virtual relationship. For the objective of estimating the total per-flow delay and jitter, it is essential to model the relationship between the flow traffic applied to propagate information through the wired medium and the links used for this purpose, as shown in the generic graph in Figure 3. This modeling step is fundamental, as the VTwin input is not the original graph representing the transport network, but rather the hypergraph derived from it. The relationship between the flows and links of Figure 3 creates an essential circular dependency that is explored to generate the heterogeneous graph used as input for the VTwin model. In this case, we can see that flow f_1 depends on links e_1 , e_2 , and e_5 . Similarly, the flow f_2 has a dependency on the links e_3 , e_4 , and e_5 . Therefore, these relationships generate the VTwin input graph depicted in Figure 4.

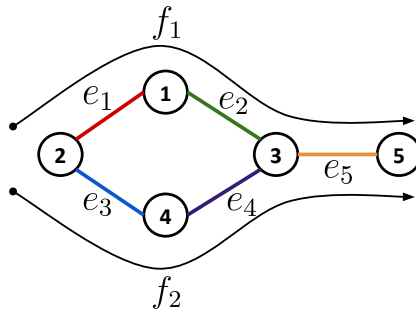


Figure 3: Links and flows relationship in a generic network topology.

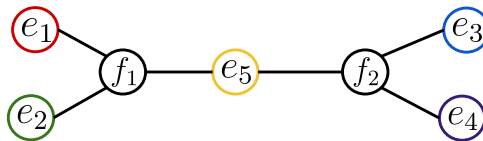


Figure 4: Heterogeneous graph, considering flow and link node types, generated from the transport network of Figure 3.

Regarding the architecture of the VTwin, we have a GNN based on a modified RouteNet-Fermi with a self-attention mechanism [33], as illustrated in Figure 5. This model processes flow and link characteristics through message passing across two gated recurrent unit (GRU)-based layers. The aggregated messages are used by a readout function defined by a MLP to compute the parameters used to estimate QoS metrics.

The embedding initialization aims to process the node features \mathbf{x}_{f_i} and \mathbf{x}_{e_j} from a heterogeneous graph obtained from the relationship between the links and the flows; that is, the f_i flows that passed through several links and the e_j links that received each flow [33]. Since this graph has two types of nodes with different feature vectors, specific embedding initialization functions are used to convert the features of each node type from their original dimensions

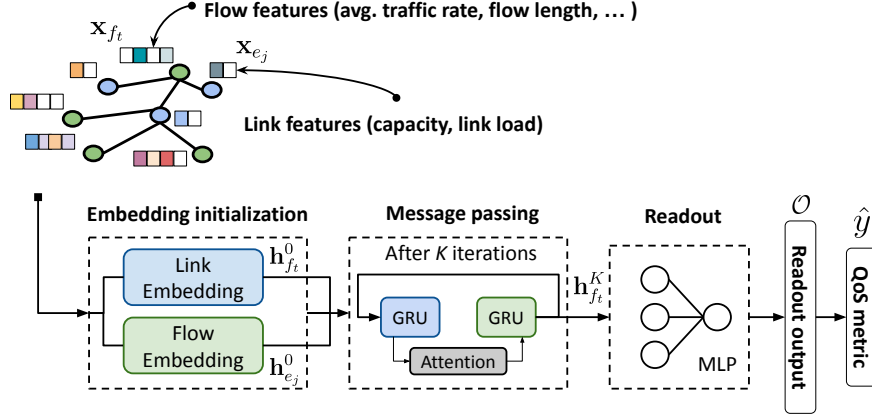


Figure 5: The adopted GNN architecture takes as input both flow and link features from the heterogeneous graph. It is composed of three modules: embedding initialization, message passing, and readout. Its output consists of QoS metrics such as delay and jitter.

to high-dimensional space $\mathbf{h}_{f_i} \in \mathbb{R}^m$, $\mathbf{h}_{e_j} \in \mathbb{R}^n$, where m and n are model hyperparameters, respectively, representing the sizes of the flow and link embedding vectors.

To obtain these high-dimensional vectors for each node type, two MLP layers are used as an initialization function, both with one hidden layer and having the output dimension defining the embedding size, $\|\mathbf{h}_{f_i}\| = m$ and $\|\mathbf{h}_{e_j}\| = n$. Thereby, this embedding initialization is defined by equations:

$$\mathbf{h}_{f_i} = \text{MLP}(\mathbf{x}_{f_i}, \theta_{f_i}), \quad (1)$$

and

$$\mathbf{h}_{e_j} = \text{MLP}(\mathbf{x}_{e_j}, \theta_{e_j}), \quad (2)$$

where θ_{f_i} , θ_{e_j} are the learnable parameters of each initialization function.

In the message-passing phase, these high-dimensional vectors are processed iteratively during $k \leq K$ (which K is another model hyperparameter) time steps by the message function $\psi(\cdot)$ and updated by functions $\phi_f(\cdot)$, $\phi_l(\cdot)$, as defined as follows [48]:

$$\mathbf{h}_{f_i}^{k+1} = \phi_f(\mathbf{h}_{f_i}^k, \psi(\mathbf{h}_{f_i}^k, \mathbf{h}_{e_j}^k)), \quad (3)$$

and

$$\mathbf{h}_{e_j}^{k+1} = \phi_l\left(\mathbf{h}_{e_j}^k, \bigoplus_{p \in \mathcal{N}_e} a(\mathbf{h}_{e_j}^k, \mathbf{h}_p^{k+1}) \psi(\mathbf{h}_{e_j}^k, \mathbf{h}_p^{k+1})\right), \quad (4)$$

where \bigoplus is an aggregation function, $a(\cdot)$ is the attention score, and \mathcal{N}_e is the neighborhood of the e -th link node. Moreover, this model treats the message function as a GRU layer, and the auxiliary assignment operation as an update function. The output of the message-passing is used by the readout function to calculate the parameter O , implemented using an MLP with two hidden layers. This MLP produces a single-neuron output, as defined by the following equation:

$$O = \text{MLP}(\mathbf{h}_{f_i}^{k+1}, \theta_o), \quad (5)$$

where θ_o are the learnable parameters of the readout MLP layer.

Considering that a flow set passes through J links, in the delay prediction task, this parameter O can be interpreted as queue occupancy, such that the predicted total per-flow delay $\hat{y}^{(\text{delay})}$ is evaluated by:

$$\hat{y}^{(\text{delay})} = \underbrace{\sum_{j=0}^J \left(\frac{O_j}{\mathcal{E}'_j} \right)}_{\text{Queue delay}} + \underbrace{\sum_{j=0}^J p_j}_{\text{Propagation delay}}. \quad (6)$$

Although no explicit variations in queue configuration (such as buffer size) are introduced, the predicted total per-flow delay \hat{y}^{delay} in Eq. (6) inherently includes the effect of queuing delay, derived using the output from Eq. (5), as the queue states implicitly affect each flow's state [11].

Finally, the predicted total per-flow jitter is directly evaluated using the output of readout function, as defined by:

$$\hat{y}^{\text{(jitter)}} = \sum_{j=0}^J \left(\frac{O_j}{\mathcal{E}'_j} \right). \quad (7)$$

3.4. NDT Synchronization

A well-defined LCM provides the NDT platform with the essential capabilities to function effectively in a production environment. It defines how the NDT should behave under various conditions, especially during the operational phase [14], whether those conditions are routine or exceptional. Consequently, all LCM phases can encompass different modules of the architecture presented in Figure 1, each of which has a specific role and lifespan to ensure the correct operation of the NDT tasks [14]. Since each phase has a different lifespan, some modules shown in Figure 1 may not exist in particular phases, as depicted in Figure 6.

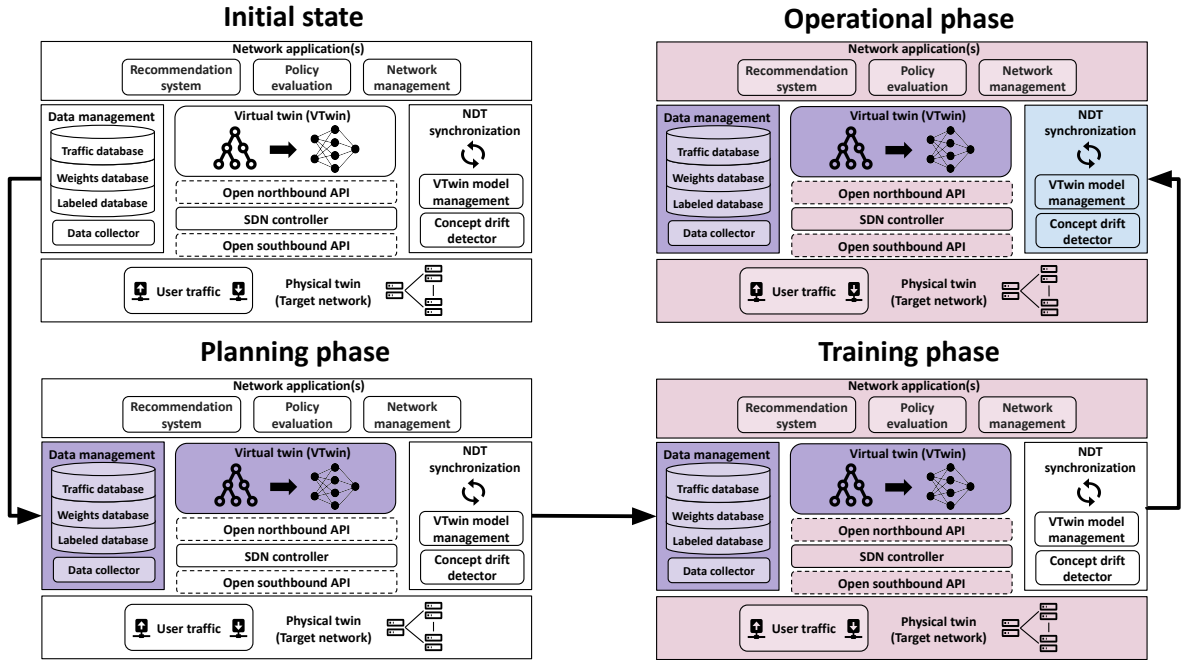


Figure 6: The NDT LCM comprises three phases: planning, training, and operational. Initially, no module is activated. During the planning phase, only the data management and VTwin modules are enabled (purple blocks). In the training phase, interaction with the PTwin by the SDN interfaces and the use of a network application are required (light magenta blocks). Finally, in the operational phase, all modules are activated, and NDT synchronization (light blue block) operates to maintain adequately the performance of the VTwin.

For instance, during the planning stage of the VTwin, the PTwin is not yet required. At this point, the VTwin can be trained using pre-existing datasets [12], considering related features from the target network environment and eliminating the need for real-time data integration. As a result, only the VTwin and selected components of the data management module are active. This phase closely resembles the process of training an AI model for predictive tasks using offline data, where the focus is on optimizing model parameters and hyperparameters based on generalization performance. Noteworthy is that the early stages of NDT for the transport network, as seen in the related works, had a specific focus during this phase. As the NDT lifecycle progresses, the training phase begins to incorporate the physical

components of the SDN infrastructure, including the interfaces connected to the SDN controller. In this context, training refers to the process of evaluating the VTwin prior to its deployment in a production environment. This phase enables the identification and mitigation of potential critical issues that could impact the proper functioning of the NDT platform. Finally, in the operational phase, we employ two submodules that monitor the synchronization states of the NDT: the concept drift detector and VTwin model management. These submodules are essential as they ensure the NDT robustness against traffic variability after NDT planning and deployment, which is intimately associated with the degree of synchronization between the VTwin and PTwin [15, 24]. This twinning rate will determine the frequency at which the NDT will start the process of synchronizing the network states of the VTwin [28].

Concept drift detector

In a data-driven supervised learning approach, the synchronization process is associated with a retraining operation [49] that can be triggered based on the input or output of the neural network model, as depicted in Figure 7a and 7b, respectively. In this context, concept drift can be detected using input features such as the average traffic rate or output features such as per-flow delay and jitter. These features may be analyzed either individually or jointly by the concept drift detector. When considered jointly, the detection relies on a multivariate concept drift detector [50], whereas analyzing each feature independently corresponds to a univariate approach.

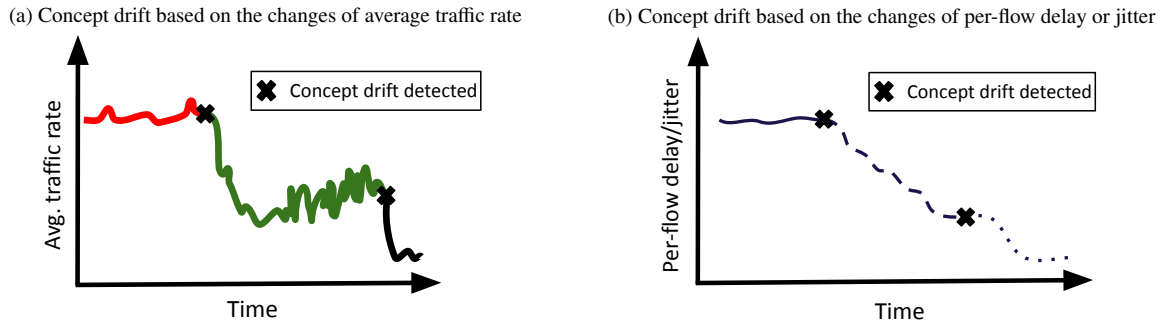


Figure 7: Types of data sources that can trigger a retraining process in a data-driven NDT.

This choice is essential, as the synchronization between the VTwin and PTwin will differ significantly depending on the target variable considered in the concept drift detection process. In the first case, synchronization is driven by the distribution pattern of each input feature, such as the network traffic of a flow passing through a set of links. In this sense, when decisions regarding concept drift are made solely based on the input data, the approach is referred to as a *distribution-based* method [51]. In contrast, when the correct labels are also considered, the method is classified as *performance-based* [51]. In the latter approach, within the context of this problem, synchronization depends on the label, specifically on the total per-flow delay or jitter. However, using this approach under realistic conditions, detecting the *aging* of a neural network model is not straightforward, as the ground truth of the QoS metric is not readily available for direct comparison with VTwin’s predictions. Therefore, our synchronization approach employs a univariate distribution-based method that monitors the average flow traffic rate to detect concept drift during the VTwin operation, thereby eliminating the need to rely on ground truth delay or jitter to trigger the synchronization process through VTwin retraining. In operational terms, to reach these synchronization steps, we need to pass through different NDT modules, as defined by the flowchart in Figure 8.

The process starts with user traffic originating from the transport network. This raw traffic data is captured by the relevant network functions and stored in the traffic database. The data collector then extracts a key feature for use by the concept drift detector: the average traffic rate of each flow. This feature is selected because it effectively captures the primary characteristic of user traffic: its average throughput. Thereby, using a univariate covariate-based method as a concept drift detector, we can identify changes in the input distribution of features over time when $P_t(x_{f_t}) \neq P_{t+w}(x_{f_{t+w}})$, where t represents a given time instant, $\{x_{f_t} \in \mathbf{x}_{f_t}, x_{f_{t+w}} \in \mathbf{x}_{f_{t+w}}\}$ is a feature in time instant t and $t + w$, in this case, the average traffic rate, and w are the sizes of the time window. In this context, our concept drift detector serves as a monitoring agent that detects changes in traffic patterns as incoming traffic is processed.

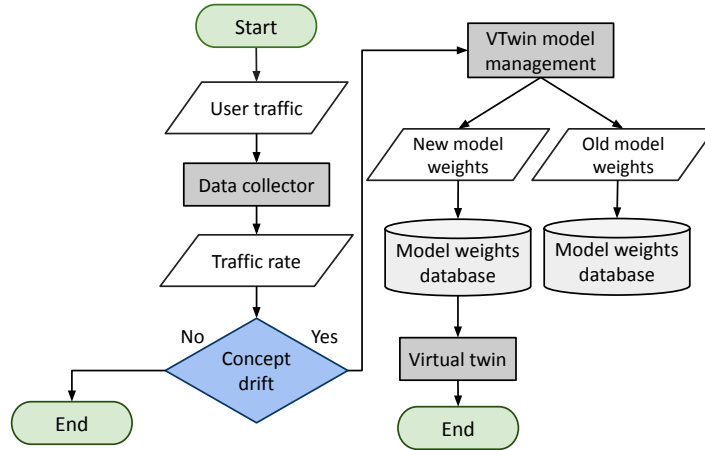


Figure 8: Sequence of steps in the operational phase to synchronize the VTwin states based on the current PTwin.

This process allows us to indirectly estimate when the total QoS metric distribution will begin to shift, signaling the expected degradation in VTwin performance and triggering retraining.

VTwin model management

When a concept drift is detected, the concept drift detector notifies the VTwin model management submodule with a warning to start retraining using data that is already available in the labeled database. Upon the start of the retraining process, the VTwin model management locks the trigger to prevent the drift detector from issuing duplicate warnings for the same drift event that has been previously addressed until the training is finished. Upon completion of the retraining process, the VTwin model management sends a control message to the VTwin, archives the previously trained model weights in a dedicated database, and updates the VTwin model with the newly learned weights.

3.5. Network application

The network application is organized to use the predictions provided to the VTwin to perform adjustments in the PTwin, considering applications that may change the state of the PTwin, such as routing optimization or flow admission control, as well as those related to the management of the network, such as SLA monitoring for *what-if* analysis [6] or emergency preparedness [52]. To achieve this, various submodules can be employed within these applications, including, but not limited to, a recommendation system to propose different configurations in the PTwin, a policy evaluation module to evaluate the configurations suggested by the recommendation system, and a network management submodule designed to provide application-level metrics from the PTwin.

Recommendation system

In scenarios where the network application aims to optimize certain states of the PTwin, this module incorporates auxiliary tools, such as a recommendation system, that assist the network operator by leveraging outputs from the VTwin. This recommendation system can generate new policies that can potentially be applied to the PTwin. For example, in routing optimization, the recommendation system, which can be based on a genetic algorithm [35] or a reinforcement learning model [4], may propose new routing policies based on total per-flow delay metrics provided by the VTwin, aimed at optimizing the QoS metrics on the transport network. Once suggested, this recommendation is sent to the policy evaluation submodule to be evaluated by a network operator if a human-in-the-loop NDT is being used [2, 4].

Policy evaluation

In a man-in-the-loop architecture, a policy evaluation submodule is essential to prevent network modifications without human oversight, which is an important safeguard in production environments, particularly in architectures

built on 5th generation (5G) networks [10]. This is especially critical given the interdependence of network components, such as the reliance of the RAN on the transport network. The role of this submodule is to consolidate all relevant information and assess the potential impacts on the network, enabling informed decision-making by the operator. Once a policy is evaluated, the final decision on its implementation rests with the operator. If approved, the corresponding control data is transmitted to the SDN controller via the northbound API and subsequently applied to the PTwin, thus completing the NDT loop.

Network management

When the application serves as a network management tool for *what-if* analysis, the task becomes conceptually simpler, as it does not require direct interaction with the PTwin to implement changes. Instead, its main objective is to provide the network operator with insight into the possible outcomes of specific scenarios or conditions [52], which can be useful in network planning tasks. This work explores a particular use case in the Experimental Results section, focusing exclusively on the network management submodule to provide SLA violations in the network [53, 54]. The selected application assesses compliance with flow SLAs, specifically detecting violations related to the packet delay budget (PDB) assigned to each packet. For example, if the total per-flow delay exceeds the PDB assigned for this flow. So, for a given set of flows that traverse the transport network, this application can estimate the number of SLA violations, relying on the total per-flow delay predictions provided by the VTwin.

4. Experiments

The PTwin integrates both emulation and simulation components used as part of the experiments to evaluate the proposed architecture. Using Mininet with the Open Network Operating System (ONOS) controller, the emulated component focuses on topology organization, while the simulated component handles traffic generation. For emulated network topologies, we use four transport networks: the 5G-Crosshaul topology [17], the PASSION project topology [17], the *Germany* topology [55], and the Synthetic-700 topology comprising networks with 128, 51, 50, and 700 nodes, respectively, each with 63, 88, 224, and 1083 links. The details about the characteristics of link capacity and link propagation delay are also described in Figures 9a and 9b, respectively.

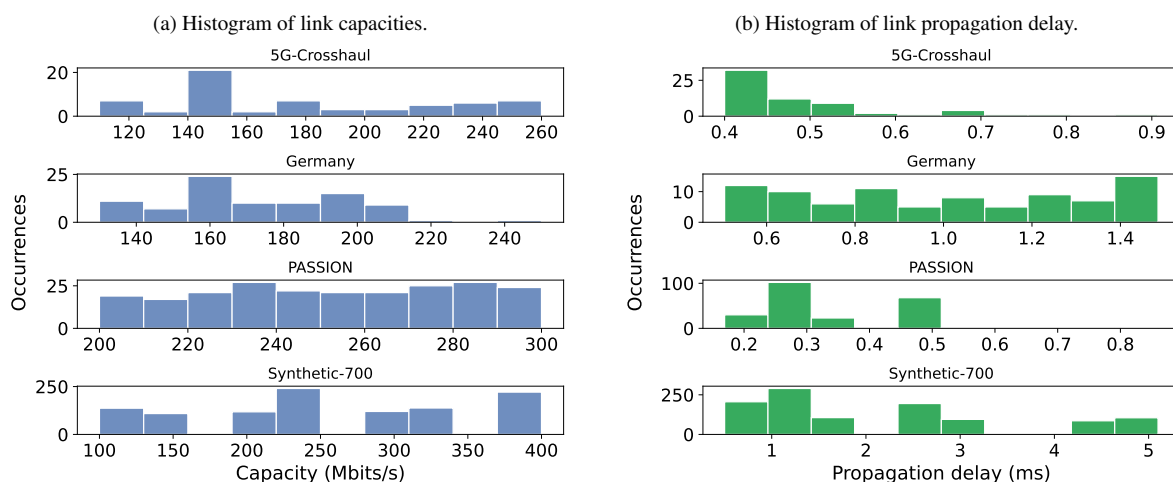


Figure 9: Link characteristics of the topologies used in our experiments.

We employ the Distributed Internet Traffic Generator (D-ITG) using a client-server model over the Transmission Control Protocol (TCP) and User Datagram Protocol (UDP) protocols to generate realistic traffic patterns. To do so, we used a computer equipped with an Intel® Core™ i7-10700F CPU @ 2.90 GHz, an NVIDIA® GeForce RTX 3060, 128 GB of RAM, and a storage capacity of 9 TB. This setup enables the incorporation of various traffic distributions within an emulation environment that is orchestrated using a suite of tools summarized in Table 4 to ensure accurate and reproducible testing conditions.

Table 4: Setup configuration used to build our PTwin.

Tools	Version
Operating system	Ubuntu 20.04
ONOS	2.6.0
Mininet	2.3.0
Open vSwitch	2.13.8
OpenFlow	1.0
D-ITG	2.8.1

We consider different distributions of packet size (in bytes) and traffic rate (in Mbits/s), without loss of generality, used to model internet traffic [56, 57], such as *Poisson*, *Exponential*, *Uniform*, and *Deterministic*, in the presence of congestion. The parameters for each are defined in Table 5, considering the minimum and maximum values $\mathcal{U}(512, 1024)$ for the uniform distribution, the mean for the exponential $\mathcal{E}(1024)$ and $\mathcal{P}(2048)$ for a Poisson distribution, as well as a deterministic pattern with traffic congestion defined by a constant value $K = 512$ for a constant packet size in traffic generation. For the packet rate, we considered the same distribution as defined for the packet size. This simplification regarding the packet rate distribution was made to maintain a controlled environment and to gain a clearer understanding of the strengths and limitations of the proposed architecture.

Table 5: Packet size distributions used to simulate user traffic.

Traffic pattern	Protocol	Packet size (bytes)
Uniform	TCP	$\mathcal{U}(512, 1024)$
Exponential	TCP	$\mathcal{E}(1024)$
Poisson	TCP	$\mathcal{P}(2048)$
Deterministic	UDP	$K = 512$

The datasets created from this traffic generation for a possible retraining process are presented in Table 6, characterized by the four distribution patterns of packet size and traffic rate, the type of topology, and the number of flows (training examples). The training examples in this case refer to the number of samples that are to be used as input-output pairs in the model retraining.

Considering these emulated environments, we propose several experiments using topologies that experience a sudden concept drift in traffic characteristics. We introduced an artificial drift at specific time intervals by altering the packet size distribution. As a result, the traffic follows the sequence of packet size and traffic rate patterns described below:

$$\text{Start} \rightarrow \boxed{\mathcal{E}} \rightarrow \boxed{\mathcal{P}} \rightarrow \boxed{\mathcal{U}} \rightarrow \boxed{K} \rightarrow \text{End}$$

For each topology, we analyzed different time intervals of network traffic. Specifically, the total times in seconds for 5G-Crosshaul, Germany, PASSION, and Synthetic-700 are 25 100 s, 24 600 s, 26 700 s, and 39 700 s, respectively. Moreover, the experiment was carried out with the understanding that we initially trained the VTwin model using traffic flows characterized by an exponential packet size distribution. The first abrupt drift is introduced by switching the packet size distribution to a Poisson model. This changing distribution behavior persists until the final phase, where the traffic pattern transitions to a constant packet size distribution, accompanied by the presence of traffic congestion. Finally, we considered the NMSE as a metric to evaluate the VTwin performance with and without NDT synchronization throughout these concept drifts, defined as:

$$\text{NMSE}^{(q)} = 10 \log_{10} \left\{ \frac{\sum_{t=1}^T (y_t^{(q)} - \hat{y}_t^{(q)})^2}{\sum_{t=1}^T (y_t^{(q)})^2} \right\}, \quad (8)$$

Table 6: Type of labeled datasets stored used to retraining the VTwin.

#	Traffic pattern	Topology	Number of flows (T)
1	Exponential	5G-Crosshaul	121 400
		Germany	129 600
		PASSION	129 600
		Synthetic-700	170 000
2	Poisson	5G-Crosshaul	113 100
		Germany	127 800
		PASSION	113 400
		Synthetic-700	194 400
3	Uniform	5G-Crosshaul	112 500
		Germany	121 400
		PASSION	112 000
		Synthetic-700	162 000
4	Deterministic	5G-Crosshaul	100 800
		Germany	61 200
		PASSION	123 200
		Synthetic-700	186 100

where $\hat{y}_t^{(q)}$ and $y_t^{(q)}$ denote, respectively, the t -th predicted and ground-truth QoS metric among T test samples. The average values were computed using a sliding window of 100 consecutive samples over time. Although other window sizes could be used, a 100-sample window offers a suitable trade-off: it provides a sufficiently narrow confidence interval for the mean while maintaining high NMSE sensitivity to short-term variations, an aspect particularly relevant during abrupt concept drift. We apply this evaluation across 10 independent realizations, aimed at obtaining an average perspective across the NDT operation in each network topology.

Using this environment, our experiments consider a distribution-based detector aimed at detecting changes in the input. We configured the concept drift detector using the Kolmogorov-Smirnov windowing (KSWIN) method [58], as implemented by the *river* library [59]. To work correctly, this method requires three hyperparameters: the *significance* level, which is a sensitive parameter that controls the probability of false positives and is represented by a value of 0.001; a window size; and a buffer for the most recent samples. The sizes of these components vary across different topologies and are determined empirically.

For the VTwin training, we used TensorFlow 2.14.0 and maintained consistency in all training parameters across all experiments. Specifically, we used a learning rate of 0.001, 50 as the maximum number of epochs (*early stopping* callbacks were also applied), applied Z-score normalization for feature scaling, adopted the *Adam* optimizer, and used Mean Absolute Percentage Error (MAPE) as the loss function. Moreover, as the model hyperparameters, we used: $T = 8$ and $\|\mathbf{h}_f\| = \|\mathbf{h}_i\| = 32$. This uniform configuration was chosen to ensure that any observed differences in model performance could be attributed solely to variations in the input data. In summary, our evaluation scenario can be described by Figure 10.

Concept drift detector configuration

We have the experiments from the KSWIN results to evaluate the proposed synchronization elements, considering the four emulated topologies and the average traffic rate in Mbits/s as the features to be tracked. Figure 11 illustrates the operation of the KSWIN detector and the location of each detected drift. For each network topology, we selected a specific window size (in seconds): 6 800 for 5G-Crosshaul, 7 000 for Germany, 6 800 for PASSION, and 10 000 for the Synthetic-700 topology. Although alternative window sizes could be explored, determining the optimal size to minimize false positives falls outside the scope of this work.

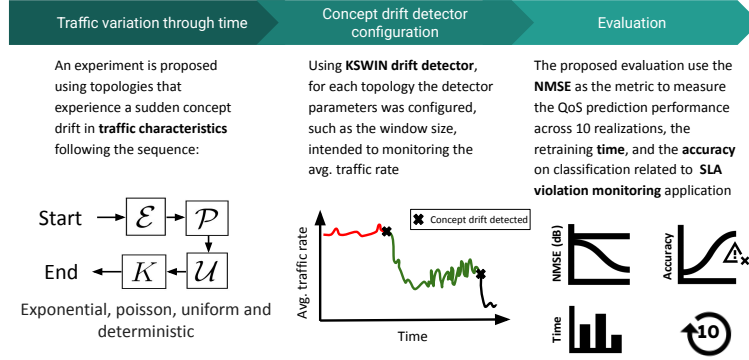


Figure 10: Experiment organization to evaluate the VTwin performance with and without synchronization in a scenario with concept drift induced by different traffic pattern.

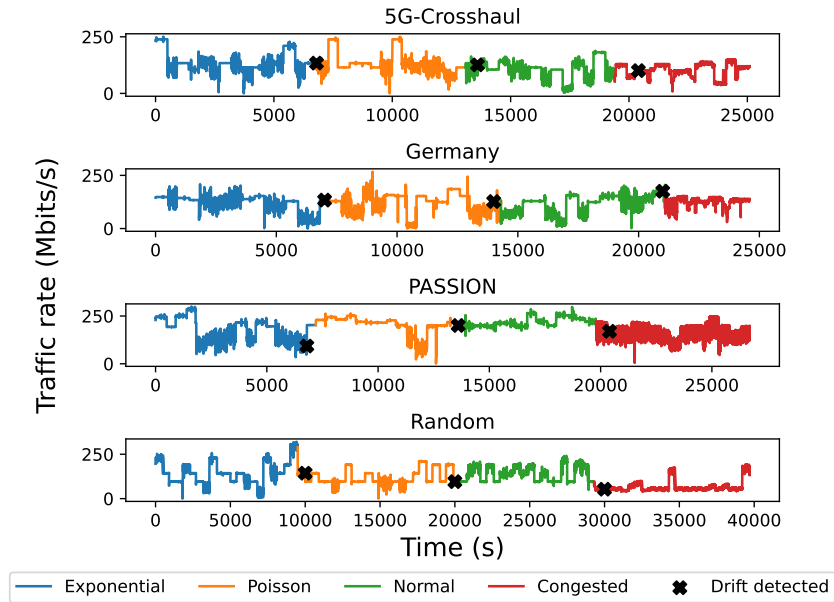


Figure 11: Drift detection pattern considering 5G-Crosshaul, Germany, PASSION, and Synthetic-700 topologies and four type of traffic patterns. Across the time series, each color in a given interval represents a different distribution pattern. The “x” points represent the detected concept drift.

In the evaluated environments, smaller window sizes generally result in a higher likelihood of false positives, as illustrated in Figure 12, which analyzes various window sizes across all topologies. The curves in this figure exhibit a consistent pattern and converge in the number of detected concept drifts as the window size increases.

Delay prediction performance

In the first experiment, we observed that concept drift was successfully detected in all instances of deviation caused by changes in the traffic pattern. However, varying detection delays were identified between the moment when the drift occurred and the moment it was detected. The resulting performance is presented in Figure 13, which shows the VTwin performance over time in the 5G-Crosshaul and Germany topology in terms of NMSE. The figure compares our proposed synchronization elements against a baseline VTwin without them, where the baseline scenario can be interpreted as one in which every concept drift results in a false negative.

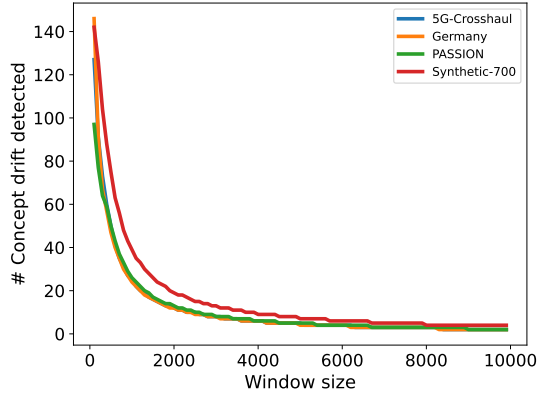


Figure 12: Relationship between the window size and the number of concept drift detection on the four topologies.

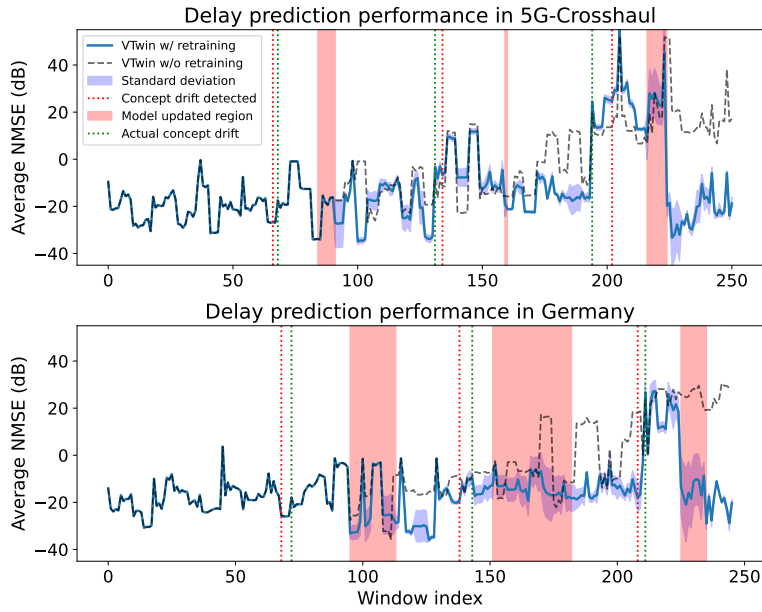


Figure 13: Validation of the proposed architecture in the 5G-Crosshaul and Germany topologies. The blue line represents the average per-flow delay prediction performance of 10 retraining realizations (in terms of NMSE) with the proposed synchronization elements. The gray dashed line shows the performance without them, and the light blue shaded area indicates the standard deviation of NMSE across all retraining realizations. Finally, the red-shaded area represents the region in which the retraining process occurred across realizations.

Before the first concept drift is detected, the VTwin operates in a typical manner, as seen in the related work: a GNN model that is already trained to generalize to unseen datasets and, based on its predictions, performs the required analysis within the proposed application. However, after the first concept drift occurs, the scenario changes due to traffic variability, leading to model degradation, evidenced by some sample windows exhibiting NMSE values near 0 dB. Despite this decline, the VTwin model remains stable, even without retraining, as the underlying data distributions, such as Poisson and Exponential, are still related. This behavior changes after the second concept drift, as the input data distribution changes to a packet size with a distinct pattern, requiring retraining, which is evident in the accentuated NMSE difference between the models with and without retraining. In the last concept drift, the VTwin becomes obsolete without a retraining process, as the input data distribution shifts to a UDP connection characterized by a constant packet size and the absence of congestion control. At this point, retraining becomes extremely necessary,

as demonstrated by the pronounced performance gap between the models with and without retraining.

The results obtained for the remaining two topologies are intended to further validate the effectiveness of the proposed synchronization method across networks with diverse characteristics in terms of scalability. Specifically, the PASSION topology comprises 128 nodes and approximately three times more links than the 5G-Crosshaul topology, while the Synthetic-700 topology contains roughly thirteen times more nodes than the Germany topology. Despite these substantial differences in scale and connectivity, Figure 14 shows consistent behavior across both topologies, comparable to that observed in the 5G-Crosshaul and Germany scenarios. In particular, during the final concept drift detected by the drift detector, the results reinforce the same conclusions regarding the necessity of mandatory retraining due to degraded VTwin prediction performance.

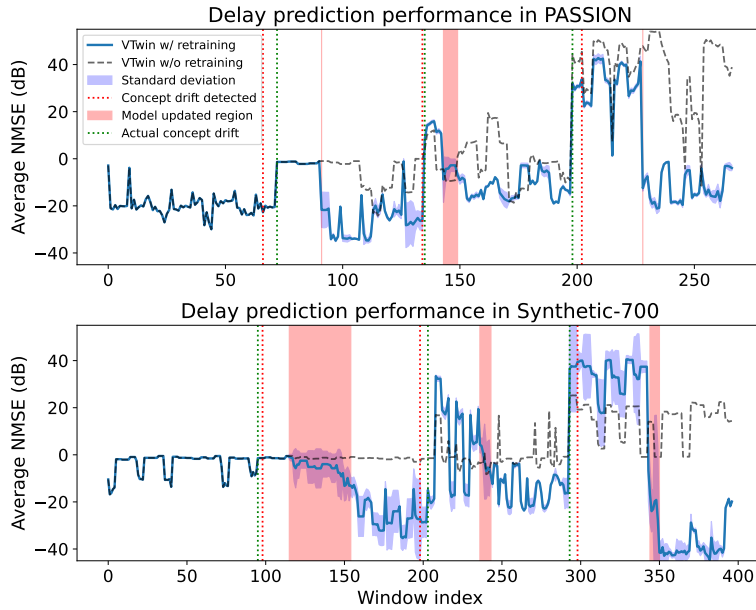


Figure 14: Comparison of the per-flow delay prediction performance using the proposed architecture considering PASSION and Synthetic-700 topologies.

In terms of retraining time cost in minutes, across these 10 realizations, we obtained the following results depicted by Figure 15. In our environment, the training time analysis shows that three out of four retraining processes for the delay prediction task are completed in less than 35 minutes. The exception is the Synthetic-700 topology, which is explained by the size of the topology. Considering the overall NDT operation time, the feasibility of the retraining duration depends on the specific application, and optimizing this time lies beyond the scope of this work. In our scenario, for instance, within the 5G-Crosshaul topology, 83.41 minutes are spent in retraining states out of a total of 418.8 minutes, corresponding to approximately 20% of the total operation time. For the Germany and PASSION topologies, the proportion of time devoted to retraining remains below 22%. Finally, for the Synthetic-700, the retraining time spent was below 32%, indicating a reasonable balance between adaptability and operational continuity.

Noteworthy, in certain concept drift events, the retraining time can be considerably shorter. For instance, in the PASSION topology, following the second detected drift, the average retraining duration was only 9.42 minutes. This reduction is primarily due to the use of an *early stopping* callback, which prevents unnecessary training of the VTwin model once convergence is reached.

Finally, Table 7 summarizes the NMSE across all window examples, highlighting VTwin’s performance before and after each concept drift. For the NMSE after the concept drift, we assume the mean average NMSE for comparison with the approach without synchronization, since our evaluation considers 10 retraining process realizations. Hence, incorporating our NDT synchronization module results in a performance improvement of at least 64% in predictions compared to configurations without it. Furthermore, given our empirical goal of achieving an average NMSE below -10 dB, the approach without NDT synchronization meets this target in only 2 of the 12 concept drifts across all

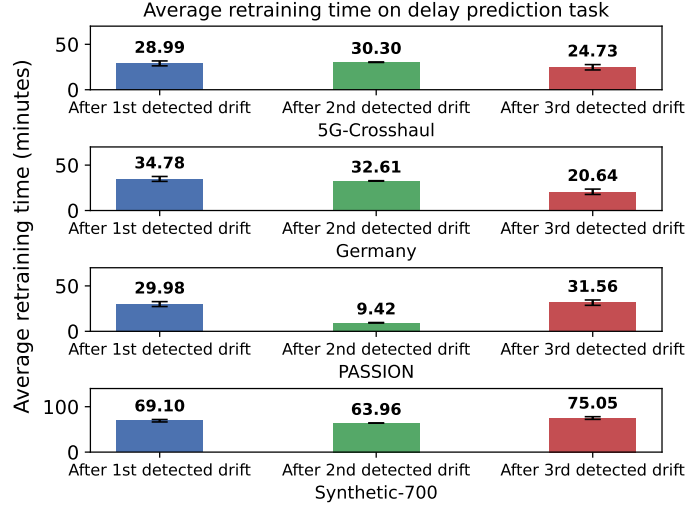


Figure 15: Average retraining time (in minutes) cost by the VTwin to synchronize with the PTwin in the delay prediction task. The value above each bar represents the average retraining time.

evaluated topologies. In contrast, our proposed approach with NDT synchronization achieves this performance in 6 out of 12 cases following concept drift. Thus, from a general perspective, for all topologies and after all concept drifts, the performance of the predictions has improved, highlighting the importance of twin synchronization in production environments where concept drift is pervasive.

Table 7: NMSE performance in predicting per-flow delay (in dB) before and after concept drift, considering the NDT operation both with and without the proposed synchronization module.

Topology	Drift ID	Pre-drift avg. NMSE w/o sync.	Post-drift avg. NMSE w/o sync.	Pre-drift mean avg. NMSE w/ sync.	Post-drift mean avg. NMSE w/ sync.
5G-Crosshaul	1	-20.69	-14.36	-20.69	-18.87
	2	-14.36	-5.11	-18.87	-10.10
	3	-5.11	17.40	-10.10	2.08
Germany	1	-18.88	-14.10	-18.88	-19.01
	2	-14.10	-1.79	-19.01	-13.82
	3	-1.79	24.64	-13.82	-3.27
PASSION	1	-19.95	-5.41	-19.95	-19.01
	2	-5.41	-1.14	-19.01	-8.06
	3	-1.14	38.09	-8.06	7.19
Synthetic-700	1	-3.76	-1.44	-3.76	-13.77
	2	-1.44	-0.93	-13.77	-6.42
	3	-0.93	14.89	-6.42	-2.05

Jitter prediction performance

Using the same environment, we also evaluated the per-flow jitter prediction performance in scenarios with and without NDT synchronization. In this sense, Figures 16 and 17 depict the performance in terms of NMSE in the 5G-Crosshaul, Germany, PASSION, and Synthetic-700 topologies. From these results, it is possible to perceive

similar trends with NDT synchronization. For example, after the third detected concept drift, the retraining process is extremely necessary.

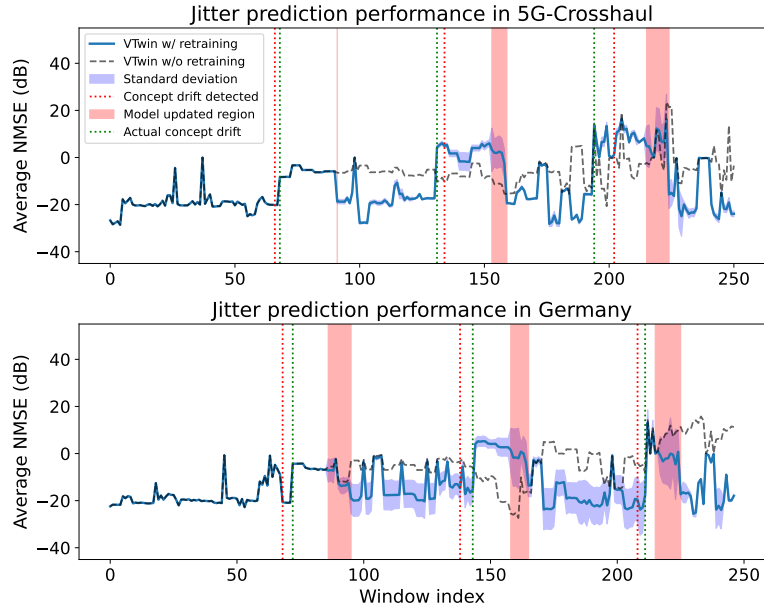


Figure 16: Comparison of the jitter prediction performance using the proposed architecture considering 5G-Crosshaul and Germany topologies.

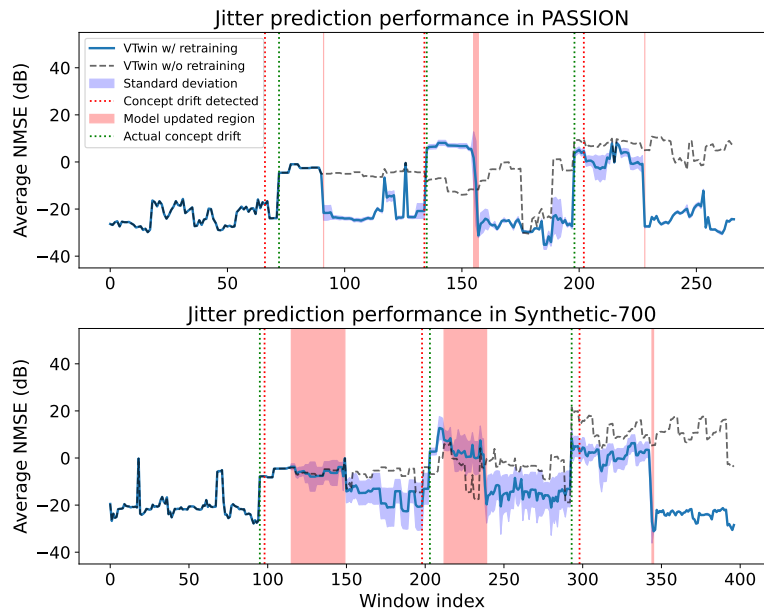


Figure 17: Comparison of the jitter prediction performance using the proposed architecture considering PASSION and Synthetic-700 topologies.

Furthermore, a similar pattern to that observed in the delay prediction training cost can be seen in the average retraining time after a concept drift event for the jitter prediction task, as shown in Figure 18. In this case, with the

exception of experiments with the Synthetic-700 topology, all retraining times remained below 35 minutes, resulting in a retraining time proportion below 20% for 5G-Crosshaul, Germany, PASSION, and below 30% for the Synthetic-700 topology.

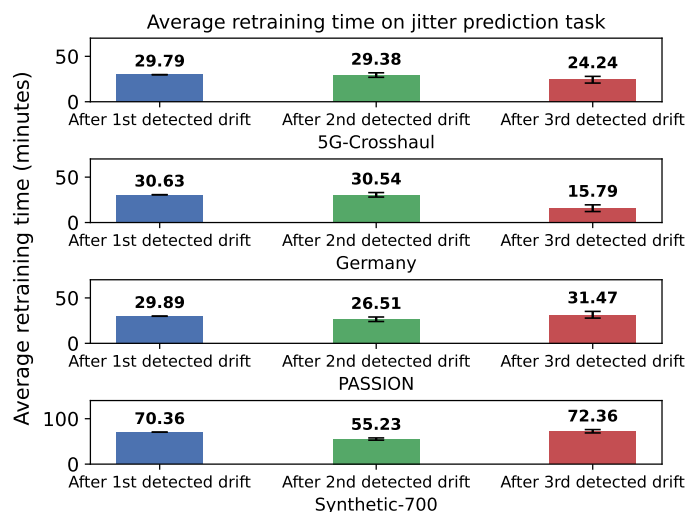


Figure 18: Average retraining time (in minutes) cost by the VTwin to synchronize with the PTwin in the jitter prediction task. The value above each bar represents the average retraining time.

These results for the jitter prediction task reaffirm the important role of the proposed NDT synchronization architecture in maintaining satisfactory performance on QoS prediction. As shown in Table 8, when using our synchronization approach, we achieved an NMSE below -10 dB in 8 out of 12 drift events, whereas the scenario without synchronization reached this level in only one event.

Table 8: NMSE performance in predicting per-flow jitter (in dB) before and after concept drift, considering the NDT operation both with and without the proposed synchronization module.

Topology	Drift ID	Pre-drift avg. NMSE w/o sync.	Post-drift avg. NMSE w/o sync.	Pre-drift mean avg. NMSE w/ sync.	Post-drift mean avg. NMSE w/ sync.
5G-Crosshaul	1	-19.78	-5.84	-19.78	-13.66
	2	-5.84	-7.60	-13.66	-8.67
	3	-7.60	-1.44	-8.67	-3.83
Germany	1	-18.30	-5.23	-18.30	-12.01
	2	-5.23	-7.63	-12.01	-11.43
	3	-7.63	7.88	-11.43	-9.46
PASSION	1	-23.10	-4.17	-23.10	-15.78
	2	-4.17	-10.32	-15.78	-15.68
	3	-10.32	6.37	-15.68	-12.98
Synthetic-700	1	-20.89	-6.39	-20.89	-11.02
	2	-6.39	-4.30	-11.02	-7.55
	3	-4.30	11.23	-7.55	-11.51

Use case with SLA violation monitoring

The use case scenario employed to evaluate the proposed NDT synchronization, considering a high-level metric related to SLA monitoring tasks, was conducted using data derived from the four topologies used in the last experiments. In this sense, we evaluated the same scenario used to validate the performance on prediction per-flow delay, but we considered high-level metrics such as the accuracy of the SLA violation predictions. In this case, we assume a simplified SLA compliance scenario, admitting only the predicted per-flow delay as the metric used to make a decision regarding the SLA violation. Thus, we assume that each flow has a specific PDB value that was assigned empirically based on the characteristics of each topology, such as the propagation delay of each link.

Regarding the experiments, we considered a total of 25 100, 24 600, 26 700, and 39 700 flows traversing the 5G-Crosshaul, Germany, PASSION, and Synthetic-700 network topologies, respectively. Each flow was evaluated by the SLA monitoring application to determine whether it was compliant with or in violation of the PDB, based on the delay predicted by the VTwin. An SLA violation occurs when the per-flow delay exceeds the PDB for the corresponding path. Table 9 summarizes the number of flows identified as being in violation for each topology.

Table 9: Flow traffic characteristics for each topology used for SLA compliance classification.

Topology	Total number of flows	Number of flows in violation
5G-Crosshaul	25 100	536
Germany	24 600	793
PASSION	26 700	1 229
Synthetic-700	39 700	1 527

The accuracy in the prediction of SLA violations is shown in Figure 19a and 19b, which considers the VTwin with and without the NDT synchronization module in the 5G-Crosshaul and Germany topologies. Each window index corresponds to the classification of 100 flows for better visualization of the results in this figure. In all topologies, the application exhibits the expected degradation in classification performance when the NDT synchronization module is disabled. This occurs because the VTwin states are not updated with those of the PTwin. Quantitatively, this results in 8 115 and 6 347 flows being incorrectly classified as compliant with their respective SLAs, in the 5G-Crosshaul and Germany topologies, respectively.

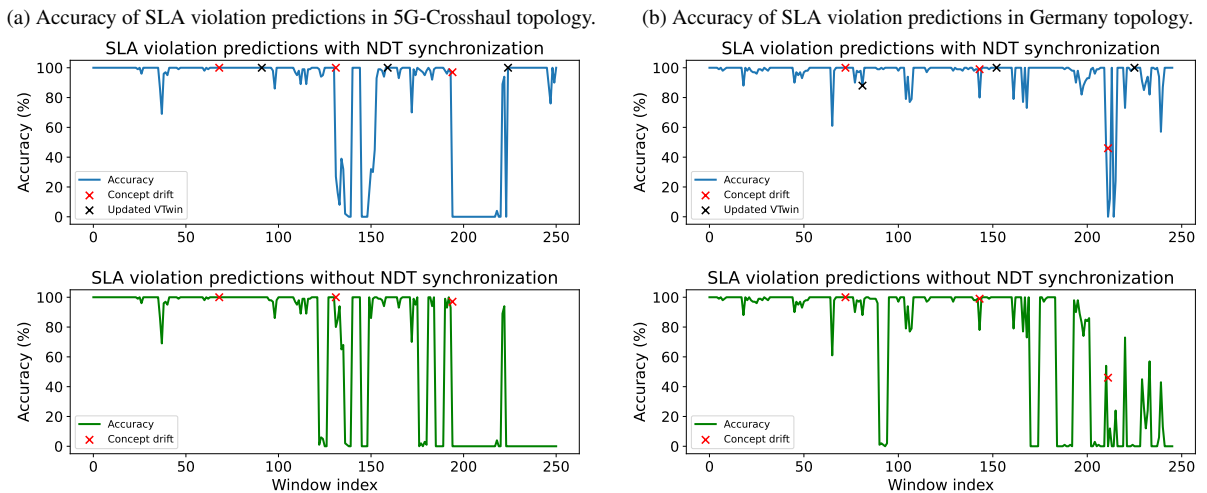


Figure 19: Accuracy of SLA violation classification considering 5G-Crosshaul and Germany topologies.

When the NDT synchronization module is enabled, however, the number of misclassified flows decreases significantly to 4 536 and 982, respectively. Similar improvements are observed in the other two topologies, as depicted

in Figure 20a and 20b, respectively, the PASSION and Synthetic-700 topologies. Moreover, all numerical results are summarized in Table 10. It is also noteworthy that part of these SLA violations occurs during periods in which the VTwin is undergoing retraining. Overall, this experiment demonstrates that the practical usability of an NDT critically depends on an effective synchronization mechanism between the twins operating at an appropriate rate, which is essential for transitioning the solution from a prototype to a production-ready framework.

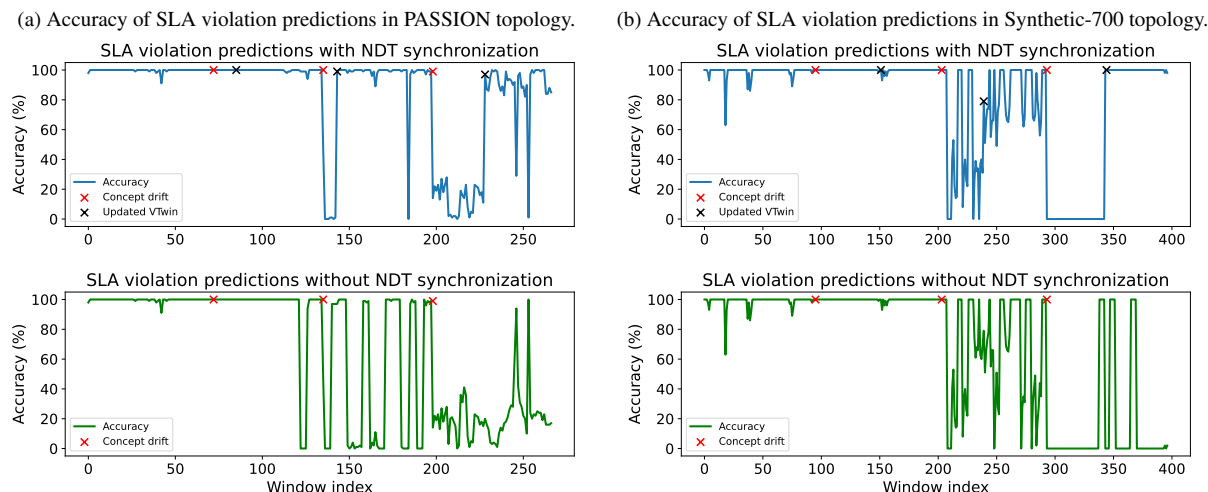


Figure 20: Accuracy of SLA violation classification considering PASSION and Synthetic-700 topologies.

Table 10: Application performance on SLA violation classification with and without NDT synchronization.

Topology	Without NDT synchronization			With NDT synchronization		
	Number of flows misclassified	Number of flows correctly classified	Accuracy (%)	Number of flows misclassified	Number of flows correctly classified	Accuracy (%)
5G-Crosshaul	8 115	16 985	67.66	4 536	20 564	81.92
Germany	6 347	18 253	74.19	982	23 618	96.00
PASSION	9 019	17 681	66.22	3 941	22 759	85.23
Synthetic-700	12 133	27 597	69.43	7 788	31 912	80.38

5. Conclusions and Future Works

This article proposed an enhanced NDT architecture incorporating data-driven synchronization modules, taking initial steps toward addressing practical and production-level aspects of NDT deployment in transport networks. The proposed modules within this architecture specifically tackle the challenge posed by the non-stationary nature of network traffic over time. In this sense, this architecture aims to ensure synchronization between the two twins of the NDT platform. To achieve this, the NDT synchronization modules, such as the concept drift detector, aim to track and detect possible changes in the traffic pattern, triggering a retraining process and ultimately updating the VTwin weights through the VTwin model management. To evaluate the architecture's operation, we considered four different topologies with sizes ranging from 50 to 700 nodes in an environment with flows using four packet size distributions, generating various traffic patterns. Thus, to detect and initiate the retraining process, we considered an input distribution-based approach, which was based on the KSWIN method. Our results demonstrate the importance of the synchronization process between the VTwin and PTwin, achieving a performance improvement in predicting total per-flow and per-flow jitter of at least 64% and 21%, respectively, compared to a configuration without a concept

drift detector. Finally, aimed at obtaining insight into the impact of the proposed NDT architecture at a high level, we also evaluated the NDT synchronization, considering an application related to SLA monitoring.

The results of the proposed experiments offer valuable insights into the challenges of twin synchronization, positioning this article as a foundational step toward future developments. A key direction for future work involves progressively incorporating more realistic elements into the experimental environments. One major limitation is the gap between the current setup and real-world production environments. Although the proposed module presents a promising approach to addressing specific challenges faced by NDT systems, it does not fully resolve all the issues required for the complete feasibility of the NDT platform. For instance, while the data management module includes essential mechanisms for collecting information from the PTwin, the experiments rely on traffic generated by a traffic generator, with metrics directly obtained from simulator logs. In contrast, data collection in a production environment is significantly more complex and may require integration with auxiliary tools, such as those defined by protocols such as the Simple Network Management Protocol (SNMP), which is used to collect network metrics. Furthermore, the feasibility of the proposed synchronization method also depends on the ability to generate synthetic data to retrain the VTwin model when necessary, which is not addressed in this article. In this context, the use of generative AI emerges as a promising solution and represents a potential avenue for future research.

In addition to addressing the data management tasks inherent to an NDT, future research will also focus on enhancing the synchronization method itself, which can be explored along two main directions. In the short term, we aim to assess synchronization performance under varying transport network conditions by adopting a more robust multivariate concept drift detection approach, one that simultaneously accounts for multiple input features, such as traffic rate, per-link load, and link capacity. Moreover, in future work, we will also consider incorporating a more realistic distribution of packet rates, as the current study assumes the same distribution for packet rate and packet size. Another aspect that should be evaluated in future work is the performance impact of the VTwin retraining process caused by false positives from these concept drift detectors, which is not addressed in this present work. In the long term, we aim to develop a more proactive synchronization strategy by integrating online learning techniques. This approach would reduce the latency in adapting the VTwin model parameters by eliminating the need to wait for explicit concept drift detection, thereby minimizing the period during which outdated model weights remain in use.

CRedit authorship contribution statement

Cláudio Modesto: Writing — original draft, Writing — review and editing, Visualization, Validation, Software, Methodology, Investigation, Data curation, Conceptualization. **João Borges:** Writing — original draft, Conceptualization. **Cleverson Nahum:** Software, Supervision, Writing – review and editing. **Lucas Matni:** Software, Formal analysis. **Cristiano Bonato Both:** Writing – review and editing, Supervision, Visualization. **Kleber Cardoso:** Writing – review and editing, Methodology. **Glauco Gonçalves:** Writing – review and editing, Formal analysis. **Ilan Correa:** Writing – review and editing. **Silvia Lins:** Writing – review and editing, Project administration. **Andrey Silva:** Writing – review and editing, Project administration. **Aldebaro Klautau:** Writing – review and editing, Project administration, Funding acquisition.

Acknowledgments

This study was financed in part by Coordenação de Aperfeiçoamento de Pessoal de Nível Superior - Brasil (CAPES) – Finance Code 001, the Conselho Nacional de Desenvolvimento Científico e Tecnológico (CNPq); the Innovation Center, Ericsson Telecomunicações Ltda., Brazil; and Project Smart 5G Core and MULTiRAn Integration (SAMURAI) (MC-TIC/CGL.br/FAPESP under grant 2020/05127-2).

References

- [1] B. R. Barricelli, E. Casiraghi, D. Fogli, A Survey on Digital Twin: Definitions, Characteristics, Applications, and Design Implications, *IEEE Access* 7 (2019) 167653–167671. doi:10.1109/ACCESS.2019.2953499.
- [2] P. Öhlén, C. Johnston, H. Olofsson, S. Terrill, F. Chernogorov, Network Digital Twins – Outlook and Opportunities, *Ericsson Technology Review* 2022 (12) (2022) 2–11. doi:10.23919/ETR.2022.9999174.

- [3] J. Suárez-Varela, P. Almasan, M. Ferriol-Galmés, K. Rusek, F. Geyer, X. Cheng, X. Shi, S. Xiao, F. Scarselli, A. Cabellos-Aparicio, P. Barlet-Ros, Graph Neural Networks for Communication Networks: Context, Use Cases and Opportunities, *IEEE Network* 37 (3) (2023) 146–153. doi:[10.1109/MNET.123.2100773](https://doi.org/10.1109/MNET.123.2100773).
- [4] R. Aben-Athar, H. Anglada, L. Costa, J. Albuquerque, A. Ferreira, C. B. Both, K. Cardoso, S. Lins, A. Silva, G. Gonçalves, I. Correa, A. Klautau, Network Digital Twin for Route Optimization in 5G/B5G Transport Slicing with What-If Analysis, in: *2025 IEEE International Conference on Communications Workshops (ICC Workshops)*, 2025, pp. 621–626. doi:[10.1109/ICCWorkshops67674.2025.11162404](https://doi.org/10.1109/ICCWorkshops67674.2025.11162404).
- [5] P. Almasan, M. Ferriol-Galmés, J. Paillisse, J. Suárez-Varela, D. Perino, D. López, A. A. P. Perales, P. Harvey, L. Ciavaglia, L. Wong, V. Ram, S. Xiao, X. Shi, X. Cheng, A. Cabellos-Aparicio, P. Barlet-Ros, Network Digital Twin: Context, Enabling Technologies, and Opportunities, *IEEE Communications Magazine* 60 (11) (2022) 22–27. doi:[10.1109/MCOM.001.2200012](https://doi.org/10.1109/MCOM.001.2200012).
- [6] H. Wang, Y. Wu, G. Min, W. Miao, A Graph Neural Network-Based Digital Twin for Network Slicing Management, *IEEE Transactions on Industrial Informatics* 18 (2) (2022) 1367–1376. doi:[10.1109/TII.2020.3047843](https://doi.org/10.1109/TII.2020.3047843).
- [7] M. Farreras, J. Paillissé, L. Fàbrega, P. Vilà, GNNNetSlice: A GNN-based Performance Model to Support Network Slicing in B5G Networks, *Comput. Commun.* 232 (C) (Mar. 2025). doi:[10.1016/j.comcom.2025.108044](https://doi.org/10.1016/j.comcom.2025.108044).
- [8] K. Rusek, J. Suárez-Varela, P. Almasan, P. Barlet-Ros, A. Cabellos-Aparicio, RouteNet: Leveraging Graph Neural Networks for Network Modeling and Optimization in SDN, *IEEE Journal on Selected Areas in Communications* 38 (10) (2020) 2260–2270. doi:[10.1109/JSAC.2020.3000405](https://doi.org/10.1109/JSAC.2020.3000405).
- [9] P. Almasan, J. Suárez-Varela, K. Rusek, P. Barlet-Ros, A. Cabellos-Aparicio, Deep Reinforcement Learning Meets Graph Neural Networks: Exploring a Routing Optimization Use Case, *Comput. Commun.* 196 (C) (2022) 184–194. doi:[10.1016/j.comcom.2022.09.029](https://doi.org/10.1016/j.comcom.2022.09.029).
- [10] S. Messaoudi, A. Ksentini, F. Messaoudi, C. Bonnet, GNN-Based SDN Admission Control in Beyond 5G Networks, in: *GLOBECOM 2023-2023 IEEE Global Communications Conference*, IEEE, 2023, pp. 6103–6108. doi:[10.1109/GLOBECOM54140.2023.10437301](https://doi.org/10.1109/GLOBECOM54140.2023.10437301).
- [11] M. Ferriol-Galmés, J. Paillisse, J. Suárez-Varela, K. Rusek, S. Xiao, X. Shi, X. Cheng, P. Barlet-Ros, A. Cabellos-Aparicio, RouteNet-Fermi: Network Modeling With Graph Neural Networks, *IEEE/ACM Transactions on Networking* 31 (6) (2023) 3080–3095. doi:[10.1109/TNET.2023.3269983](https://doi.org/10.1109/TNET.2023.3269983).
- [12] L. Bariah, M. Debbah, The Interplay of AI and Digital Twin: Bridging the Gap Between Data-Driven and Model-Driven Approaches, *IEEE Wireless Communications* (2024). doi:[10.1109/MWC.133.2200447](https://doi.org/10.1109/MWC.133.2200447).
- [13] H. Ahmadi, A. Nag, Z. Khar, K. Sayrafian, S. Rahardja, Networked Twins and Twins of Networks: An Overview on the Relationship Between Digital Twins and 6G, *IEEE Communications Standards Magazine* 5 (4) (2021) 154–160. doi:[10.1109/MCOMSTD.0001.2000041](https://doi.org/10.1109/MCOMSTD.0001.2000041).
- [14] M. Kherbache, M. Maimour, E. Rondeau, When Digital Twin Meets Network Softwarization in the Industrial IoT: Real-Time Requirements Case Study, *Sensors* 21 (24) (2021). doi:[10.3390/s21248194](https://doi.org/10.3390/s21248194).
- [15] W. Alghamdi, E. Albassam, Synchronization Patterns for Digital Twin Systems, *Journal of Applied Data Sciences* 5 (3) (2024) 1026–1037. doi:[10.47738/jads.v5i3.267](https://doi.org/10.47738/jads.v5i3.267).
- [16] K. Hribernik, G. Cabri, F. Mandreoli, G. Mentzas, Autonomous, Context-aware, Adaptive Digital Twins—State of the Art and Roadmap, *Computers in Industry* 133 (2021) 103508. doi:<https://doi.org/10.1016/j.compind.2021.103508>.
- [17] F. Z. Morais, G. M. F. de Almeida, L. Pinto, K. V. Cardoso, L. M. Contreras, R. d. R. Righi, C. B. Both, PlaceRAN: Optimal Placement of Virtualized Network Functions in Beyond 5G Radio Access Networks, *IEEE Transactions on Mobile Computing* 22 (9) (2023) 5434–5448. doi:[10.1109/TMC.2022.3171525](https://doi.org/10.1109/TMC.2022.3171525).

- [18] L. Baier, T. Schlör, J. Schoeffer, N. Kühn, Detecting Concept Drift with Neural Network Model Uncertainty, in: T. Bui (Ed.), Proceedings of the 56th Hawaii International Conference on System Sciences, 2023, pp. 835 – 844.
- [19] M. Ameer, B. Brikauthorrefmark, A. Ksentini, Dual Self-Attention is what You Need for Model Drift Detection in 6G Networks, IEEE Transactions on Machine Learning in Communications and Networking (2025) 1–1 [doi:10.1109/TMLCN.2025.3576727](https://doi.org/10.1109/TMLCN.2025.3576727).
- [20] H. X. Nguyen, R. Trestian, D. To, M. Tatipamula, Digital Twin for 5G and Beyond, IEEE Communications Magazine 59 (2) (2021) 10–15. [doi:10.1109/MCOM.001.2000343](https://doi.org/10.1109/MCOM.001.2000343).
- [21] L. U. Khan, W. Saad, D. Niyato, Z. Han, C. S. Hong, Digital-twin-enabled 6G: Vision, Architectural Trends, and Future Directions, IEEE Communications Magazine 60 (1) (2022) 74–80. [doi:10.1109/MCOM.001.21143](https://doi.org/10.1109/MCOM.001.21143).
- [22] Z. Tao, W. Xu, Y. Huang, X. Wang, X. You, Wireless Network Digital Twin for 6G: Generative AI as a Key Enabler, IEEE Wireless Communications 31 (4) (2024) 24–31. [doi:10.1109/MWC.002.2300564](https://doi.org/10.1109/MWC.002.2300564).
- [23] M. Sheraz, T. C. Chuah, Y. L. Lee, M. M. Alam, Z. Han, et al., A Comprehensive Survey on Revolutionizing Connectivity Through Artificial Intelligence-Enabled Digital Twin Network in 6G, IEEE Access (2024). [doi:10.1109/ACCESS.2024.3384272](https://doi.org/10.1109/ACCESS.2024.3384272).
- [24] W. Liu, Y. Fu, Z. Shi, H. Wang, When Digital Twin Meets 6G: Concepts, Obstacles, and Research Prospects, IEEE Communications Magazine (2024). [doi:10.1109/MCOM.001.2400202](https://doi.org/10.1109/MCOM.001.2400202).
- [25] Recommendation ITU-T Y.3090 (2022), Digital twin network – Requirements and architecture (2022).
- [26] C. Zhou, H. Yang, X. Duan, D. Lopez, A. Pastor, Q. Wu, M. Boucadair, C. Jacquenet, Network Digital Twin: Concepts and Reference Architecture, Internet-Draft draft-irtf-nmrg-network-digital-twin-arch-10, Internet Engineering Task Force, work in Progress (Feb. 2025).
- [27] O-RAN ALLIANCE, Research reports — o-ran.org, <https://www.o-ran.org/research-reports>, [Accessed 12-12-2024] (2024).
- [28] D. Jones, C. Snider, A. Nassehi, J. Yon, B. Hicks, Characterising the Digital Twin: A Systematic Literature Review, CIRP Journal of Manufacturing Science and Technology 29 (2020) 36–52. [doi:https://doi.org/10.1016/j.cirpj.2020.02.002](https://doi.org/10.1016/j.cirpj.2020.02.002).
- [29] M. Happ, M. Herlich, C. Maier, J. L. Du, P. Dorfinger, Graph-neural-network-based Delay Estimation for Communication Networks with Heterogeneous Scheduling Policies, ITU Journal on Future and Evolving Technologies 2 (4) (2021) 1–8. [doi:https://doi.org/10.52953/TEJX5530](https://doi.org/10.52953/TEJX5530).
- [30] M. Saravanan, P. S. Kumar, A. R. Kumar, Enabling Network Digital Twin to Improve QoS Performance in Communication Networks, in: 2022 IEEE Smartworld, Ubiquitous Intelligence & Computing, Scalable Computing & Communications, Digital Twin, Privacy Computing, Metaverse, Autonomous & Trusted Vehicles (SmartWorld/UIC/ScalCom/DigitalTwin/PriComp/Meta), IEEE, 2022, pp. 2151–2160.
- [31] M. Farreras, P. Soto, M. Camelo, L. Fàbrega, P. Vilà, Improving Network Delay Predictions Using GNNs, Journal of Network and System Management 31 (4) (Oct. 2023). [doi:10.1007/s10922-023-09758-9](https://doi.org/10.1007/s10922-023-09758-9).
- [32] B. Li, T. Efimov, A. Kumar, J. Cortes, G. Verma, A. Swami, S. Segarra, Learnable Digital Twin for Efficient Wireless Network Evaluation, in: MILCOM 2023-2023 IEEE Military Communications Conference (MILCOM), IEEE, 2023, pp. 661–666. [doi:10.1109/MILCOM58377.2023.10356320](https://doi.org/10.1109/MILCOM58377.2023.10356320).
- [33] C. Modesto, R. Aben-Athar, A. Silva, S. Lins, Glauco Gonçalves, A. Klautau, Delay Estimation Based on Multiple Stage Message Passing With Attention Mechanism Using a Real Network Communication Dataset, ITU Journal on Future and Evolving Technologies 5 (4) (2024) 465–477. [doi:10.52953/RBNE4256](https://doi.org/10.52953/RBNE4256).
- [34] J. Lu, A. Liu, F. Dong, F. Gu, J. Gama, G. Zhang, Learning Under Concept Drift: A review, IEEE Transactions on Knowledge and Data Engineering 31 (12) (2018) 2346–2363. [doi:10.1109/TKDE.2018.2876857](https://doi.org/10.1109/TKDE.2018.2876857).

- [35] M. Zalat, M. Davoudzade, C. Barber, D. Krauss, B. Esfandiari, T. Kunz, A Practical Network Digital Twin for IGP Weight Optimization, in: 2024 20th International Conference on Network and Service Management (CNSM), 2024, pp. 1–7. doi:10.23919/CNSM62983.2024.10814633.
- [36] Mininet Project Contributors, Mininet: An Instant Virtual Network on Your Laptop (or Other PC) - Mininet — mininet.org, <http://mininet.org/>, [Accessed 04-12-2024] (2024).
- [37] M. Ferriol-Galmés, X. Cheng, X. Shi, S. Xiao, P. Barlet-Ros, A. Cabellos-Aparicio, FlowDT: A Flow-Aware Digital Twin for Computer Networks, in: ICASSP 2022-2022 IEEE International Conference on Acoustics, Speech and Signal Processing (ICASSP), IEEE, 2022, pp. 8907–8911. doi:10.1109/ICASSP43922.2022.9746953.
- [38] J. Lai, Z. Chen, J. Zhu, W. Ma, L. Gan, S. Xie, G. Li, Deep Learning Based Traffic Prediction Method for Digital Twin Network, Cognitive Computation 15 (5) (2023) 1748–1766. doi:10.1007/s12559-023-10136-5.
- [39] H. Shin, S. Oh, A. Isah, I. Aliyu, J. Park, J. Kim, Network Traffic Prediction Model in a Data-Driven Digital Twin Network Architecture, Electronics 12 (18) (2023) 3957. doi:https://doi.org/10.3390/electronics12183957.
- [40] P. Yu, J. Zhang, H. Fang, W. Li, L. Feng, F. Zhou, P. Xiao, S. Guo, Digital Twin Driven Service Self-healing With Graph Neural Networks in 6G Edge Networks, IEEE Journal on Selected Areas in Communications (2023). doi:10.1109/JSAC.2023.3310063.
- [41] A. Varga, The OMNET++ Discrete Event Simulation System, Proc. ESM'2001 9 (01 2001).
- [42] P. Kathiravelu, P. Van Roy, L. Veiga, SD-CPS: Software-defined Cyber-physical Systems. Taming the Challenges of CPS with Workflows at the Edge, Cluster Computing 22 (3) (2019) 661–677.
- [43] Y. Wu, K. Zhang, Y. Zhang, Digital Twin Networks: A Survey, IEEE Internet of Things Journal 8 (18) (2021) 13789–13804. doi:10.1109/JIOT.2021.3079510.
- [44] C. Güemes-Palau, P. Almasan, S. Xiao, X. Cheng, X. Shi, P. Barlet-Ros, A. Cabellos-Aparicio, Accelerating Deep Reinforcement Learning for Digital Twin Network Optimization with Evolutionary Strategies, in: NOMS 2022-2022 IEEE/IFIP Network Operations and Management Symposium, 2022, pp. 1–5. doi:10.1109/NOMS54207.2022.9789945.
- [45] D. Kreutz, F. M. V. Ramos, P. E. Veríssimo, C. E. Rothenberg, S. Azodolmolky, S. Uhlig, Software-Defined Networking: A Comprehensive Survey, Proceedings of the IEEE 103 (1) (2015) 14–76. doi:10.1109/JPROC.2014.2371999.
- [46] E. Molina, E. Jacob, Software-defined Networking in Cyber-Physical Systems: A Survey, Computers & Electrical Engineering 66 (2018) 407–419. doi:https://doi.org/10.1016/j.compeleceng.2017.05.013.
- [47] L. E. Salazar, A. A. Cardenas, Enhancing the Resiliency of Cyber-Physical Systems with Software-Defined Networks, in: Proceedings of the ACM Workshop on Cyber-Physical Systems Security & Privacy, CPS-SPC'19, Association for Computing Machinery, New York, NY, USA, 2019, p. 15–26. doi:10.1145/3338499.3357356.
- [48] M. M. Bronstein, J. Bruna, T. Cohen, P. Velivcković, Geometric Deep Learning: Grids, Groups, Graphs, Geodesics, and Gauges, ArXiv abs/2104.13478 (2021). doi:10.48550/arXiv.2104.13478.
- [49] S. S. Bagui, M. P. Khan, C. Valmyr, S. C. Bagui, D. Mink, Model Retraining upon Concept Drift Detection in Network Traffic Big Data, Future Internet 17 (8) (2025). doi:10.3390/fi17080328.
- [50] D. Lukats, O. Zielinski, A. Hahn, F. Stahl, A Benchmark and Survey of Fully Unsupervised Concept Drift Detectors on Real-world Data Streams, International Journal of Data Science and Analytics 19 (1) (2025) 1–31. doi:https://doi.org/10.1007/s41060-024-00620-y.

- [51] F. Bayram, B. S. Ahmed, A. Kessler, From Concept Drift to Model Degradation: An Overview on Performance-aware Drift Detectors, *Knowledge-Based Systems* 245 (2022) 108632. doi:<https://doi.org/10.1016/j.knosys.2022.108632>.
- [52] 3GPP, 3rd Generation Partnership Project; Technical Specification Group Services and System Aspects; Management and orchestration; Study on Management Aspect of Network Digital Twin (Release 19), Tech. Rep. TR 28.915 V19.0.0 (2024-12), 3GPP (2024).
- [53] S. U. Khan, B. Nazir, M. Hanif, A. Ali, S. Alam, U. Habib, Adaptive Runtime Monitoring of Service Level Agreement Violations in Cloud Computing, *Computers, Materials and Continua* 71 (3) (2022) 4199–4220. doi:<https://doi.org/10.32604/cmc.2022.020852>.
- [54] J. Sommers, P. Barford, N. Duffield, A. Ron, Multiobjective Monitoring for SLA Compliance, *IEEE/ACM Transactions on Networking* 18 (2) (2010) 652–665. doi:[10.1109/TNET.2009.2031974](https://doi.org/10.1109/TNET.2009.2031974).
- [55] Unviersitat Politècnica da Catalunya, Knowledge-Defined Networking Training Datasets, <https://www.knowledgedefinednetworking.org/>, [Accessed 09-01-2025] (2025).
- [56] P. Jurkiewicz, G. Rzym, P. Boryło, Flow Length and Size Distributions in Campus Internet Traffic, *Computer Communications* 167 (2021) 15–30. doi:[10.1016/j.comcom.2020.12.016](https://doi.org/10.1016/j.comcom.2020.12.016).
- [57] S. Luo, G. Marin, Realistic Internet Traffic Simulation Through Mixture Modeling and a Case Study, in: *Proceedings of the Winter Simulation Conference, 2005.*, 2005, pp. 9 pp.–. doi:[10.1109/WSC.2005.1574533](https://doi.org/10.1109/WSC.2005.1574533).
- [58] C. Raab, M. Heusinger, F.-M. Schleif, Reactive Soft Prototype Computing for Concept Drift Streams, *Neurocomputing* 416 (2020) 340–351. doi:<https://doi.org/10.1016/j.neucom.2019.11.111>.
- [59] J. Montiel, M. Halford, S. M. Mastelini, G. Bolmier, R. Sourty, R. Vaysse, A. Zouitine, H. M. Gomes, J. Read, T. Abdessalem, et al., River: Machine Learning for Streaming Data in Python, *Journal of Machine Learning Research* 22 (110) (2021) 1–8.